

# Mechano-photoexcitation for organic synthesis using mechanoluminescent materials as photon sources

Received: 7 June 2024

Accepted: 14 October 2024

Published online: 14 November 2024

 Check for updates

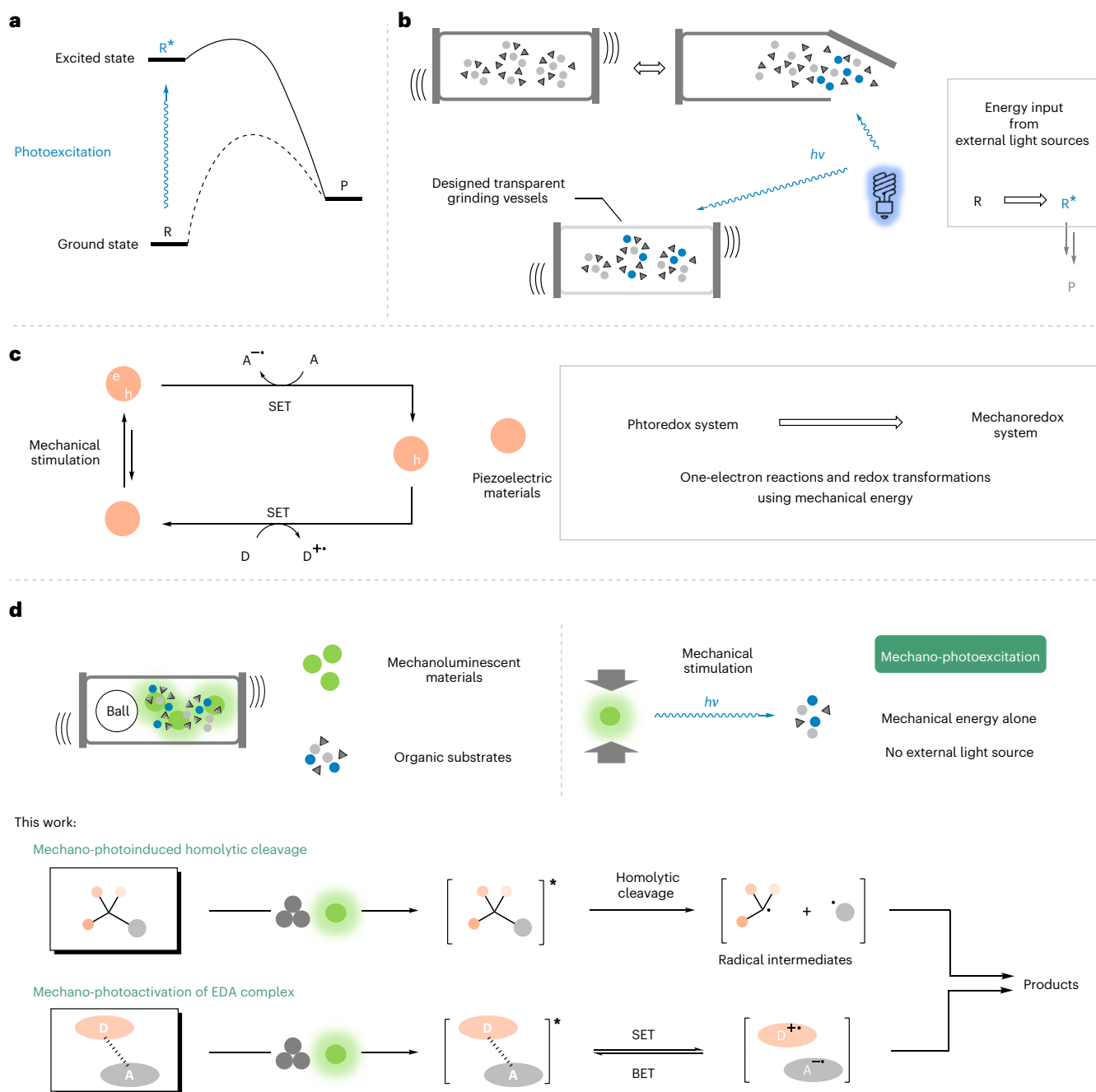
Xiaohua Xin<sup>1,4</sup>, Jinxing Geng<sup>1,4</sup>, Duo Zhang<sup>2</sup>, Hwee Ting Ang<sup>3</sup>, Hui Wang<sup>1</sup>, Yongliang Cheng<sup>1</sup>, Yun Liu<sup>1</sup>, Ren Wei Toh<sup>3</sup>, Jie Wu<sup>3</sup> & Han Wang<sup>1</sup>

Implementing photochemical reactions through mechanochemical methods can reduce waste generation by eliminating the need for bulk solvents. The absence of solvent results in exceptionally high concentrations of catalysts and reactants in reactions, substantially improving reaction rates and efficiency in terms of both time and energy utilization. However, the integration of mechano- and photochemical approaches is often hindered by the limited transparency of mechanochemical reaction vessels. Here we present a mechano-photoexcitation strategy that utilizes mechanoluminescent materials, in particular  $\text{SrAl}_2\text{O}_4:\text{Eu}^{2+}/\text{Dy}^{3+}$ , as internal photon sources activated by mechanical energy. We demonstrate the efficacy of this strategy in two photochemical processes: the Hofmann–Löffler–Freytag reaction and the activation of electron donor–acceptor complexes in sulfonylation reactions. Mechanistic studies confirm the radical nature of these transformations, and control experiments validate the critical role of mechano-photoactivation. By utilizing mechanical energy alone, this method eliminates the need for external light sources and enables gramme-scale photochemical transformations. Our approach represents a valuable application of mechanical energy in synthetic chemistry, providing a complementary means for integrating photochemistry with mechanochemistry.

Photoexcitation has substantially expanded the horizon of organic synthesis by enabling the generation of higher-energy excited-state molecules under mild conditions upon photon absorption. These excited molecules exhibit markedly distinct chemical properties and reactivity compared with their ground-state counterparts, enabling reactions that are otherwise challenging to achieve with ground-state molecules through purely thermal processes (Fig. 1a)<sup>1</sup>. This aspect of photoexcitation has attracted considerable interest among synthetic chemists, fuelling the growth of light-harnessing reactions in recent decades<sup>2–5</sup>.

Meanwhile, mechanochemistry has recently emerged as a promising approach in sustainable synthesis, offering opportunities to reduce or eliminate solvent usage and enhance environmental sustainability. By leveraging mechanical force to drive reactions, mechanochemical synthesis enables efficient utilization of solid substrates for reactions and facilitates processes that are challenging to achieve by traditional batch solution synthesis<sup>6–18</sup>. In recent years, mechanochemistry has evolved significantly by integrating external energy sources (for example, thermal, ultrasonic, electrical and light), giving rise to thermo-, sono-, electro- and photo-mechanochemistry subfields<sup>6</sup>.

<sup>1</sup>College of Chemistry & Materials Science, Northwest University, Xi'an, P. R. China. <sup>2</sup>Medicine Center, Guangxi University of Science and Technology, Liuzhou, P. R. China. <sup>3</sup>Department of Chemistry, National University of Singapore, Singapore, Republic of Singapore. <sup>4</sup>These authors contributed equally: Xiaohua Xin, Jinxing Geng. ✉ e-mail: [chmjie@nus.edu.sg](mailto:chmjie@nus.edu.sg); [hanwang@nwu.edu.cn](mailto:hanwang@nwu.edu.cn)

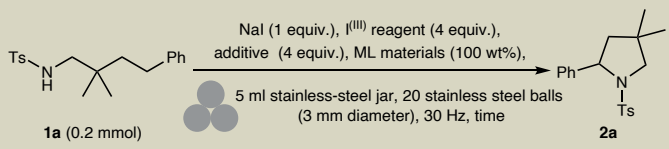


**Fig. 1 | Achieving or simulating photochemical transformations in mechanochemistry.** **a**, Photoexcitation. **b**, Combination of irradiation and grinding. **c**, Mechanoredox system with piezoelectric materials. **d**, Mechano-photoexcitation using ML materials. BET, back-electron transfer; A, acceptor; D, donor; R, reagent; P, product; e, electron; h, hole.

This expansion has further broadened its application scope and enhanced its efficiency.

Photo-mechanochemistry, a highly promising subfield in sustainable chemistry, has received less attention than its counterparts, primarily due to challenges in effectively irradiating reactions with light sources. The typical opacity of commercially available mechanochemical equipment necessitates separate mechanical activation and photoactivation steps (Fig. 1b)<sup>19–22</sup>. Alternatively, custom-built transparent grinding vessels are required to enable irradiation penetration from external light sources during the reaction<sup>23–30</sup>. Hence, there is a pressing need for the development of new approaches in photo-mechanochemistry that circumvent such limitations. An important breakthrough has been achieved through the utilization

of piezoelectric materials, which generate an electric charge under mechanical stress, thus promoting single-electron transfer (SET) processes for the redox activation of molecules during synthesis (Fig. 1c)<sup>31–34</sup>. This innovation has resulted in mechanoredox systems emerging as a viable alternative to the well-established photoredox system, advancing the field of mechanochemistry. Such advancements provide fresh research perspectives and tools for integrating solid-state photoreactions with mechanochemical methods. However, beyond photoredox processes, the use of solely mechanical energy to achieve or simulate other types of photochemical transformations, such as photoinduced homolysis and photoactivation of electron donor–acceptor (EDA) complexes, remains unexplored.

**Table 1 | Optimization for mechanical HLF reaction**


Entry <sup>a</sup>	ML materials	I <sup>(III)</sup> reagent	Additive	Time	Yield (%) <sup>b</sup>
1	ZnS:Cu <sup>+</sup>	PhI(OCOCF <sub>3</sub> ) <sub>2</sub>	–	90 min	16
2	SrAl <sub>2</sub> O <sub>4</sub> :Eu <sup>2+</sup>	PhI(OCOCF <sub>3</sub> ) <sub>2</sub>	–	90 min	44
3	SrAl <sub>2</sub> O <sub>4</sub> :Eu <sup>2+</sup> /Dy <sup>3+</sup>	PhI(OCOCF <sub>3</sub> ) <sub>2</sub>	–	90 min	49
4	Sr <sub>2</sub> MgSi <sub>2</sub> O <sub>7</sub> :Eu <sup>2+</sup> /Dy <sup>3+</sup>	PhI(OCOCF <sub>3</sub> ) <sub>2</sub>	–	90 min	37
5	SrSi <sub>2</sub> O <sub>2</sub> N <sub>2</sub> :Eu <sup>2+</sup>	PhI(OCOCF <sub>3</sub> ) <sub>2</sub>	–	90 min	22
6	BaSi <sub>2</sub> O <sub>2</sub> N <sub>2</sub> :Eu <sup>2+</sup>	PhI(OCOCF <sub>3</sub> ) <sub>2</sub>	–	90 min	32
7	SrAl <sub>2</sub> O <sub>4</sub> :Eu <sup>2+</sup> /Dy <sup>3+</sup>	PhI(OAc) <sub>2</sub>	–	90 min	Trace
8	SrAl <sub>2</sub> O <sub>4</sub> :Eu <sup>2+</sup> /Dy <sup>3+</sup>	PhI(OH)OTs	–	90 min	63
9	SrAl <sub>2</sub> O <sub>4</sub> :Eu <sup>2+</sup> /Dy <sup>3+</sup>	PhIO	–	90 min	7
10	SrAl <sub>2</sub> O <sub>4</sub> :Eu <sup>2+</sup> /Dy <sup>3+</sup>	PhI(OH)OTs	Na <sub>2</sub> CO <sub>3</sub>	90 min	84
11	SrAl <sub>2</sub> O <sub>4</sub> :Eu <sup>2+</sup> /Dy <sup>3+</sup>	PhI(OH)OTs	SiO <sub>2</sub>	90 min	13
12	SrAl <sub>2</sub> O <sub>4</sub> :Eu <sup>2+</sup> /Dy <sup>3+</sup>	PhI(OH)OTs	Al <sub>2</sub> O <sub>3</sub>	90 min	16
13 <sup>c</sup>	SrAl <sub>2</sub> O <sub>4</sub> :Eu <sup>2+</sup> /Dy <sup>3+</sup>	PhI(OH)OTs	Na <sub>2</sub> CO <sub>3</sub>	90 min	75
14 <sup>d</sup>	SrAl <sub>2</sub> O <sub>4</sub> :Eu <sup>2+</sup> /Dy <sup>3+</sup>	PhI(OH)OTs	Na <sub>2</sub> CO <sub>3</sub>	90 min	12
15	SrAl <sub>2</sub> O <sub>4</sub> :Eu <sup>2+</sup> /Dy <sup>3+</sup>	PhI(OH)OTs	Na <sub>2</sub> CO <sub>3</sub>	60 min	32
16	SrAl <sub>2</sub> O <sub>4</sub> :Eu <sup>2+</sup> /Dy <sup>3+</sup>	PhI(OH)OTs	Na <sub>2</sub> CO <sub>3</sub>	120 min	62
17 <sup>e</sup>	SrAl <sub>2</sub> O <sub>4</sub> :Eu <sup>2+</sup> /Dy <sup>3+</sup>	PhI(OH)OTs	Na <sub>2</sub> CO <sub>3</sub>	4×30 min	90
18	–	PhI(OH)OTs	Na <sub>2</sub> CO <sub>3</sub>	4×30 min	9
19 <sup>f</sup>	–	PhI(OH)OTs	Na <sub>2</sub> CO <sub>3</sub>	4×30 min	ND (88) <sup>g</sup>

<sup>a</sup>Reaction conditions: **1a** (0.2 mmol), Nal (0.2 mmol) and I<sup>(III)</sup> reagent (0.8 mmol), ML materials (100 wt%) and the additive were charged inside a 5 ml stainless-steel milling jar using 20 3-mm-diameter stainless-steel balls and milled at 30 Hz for 90 min. <sup>b</sup>Isolated yield. <sup>c</sup>Five 5-mm-diameter stainless-steel balls were used. <sup>d</sup>One 9-mm-diameter stainless-steel ball was used.

<sup>e</sup>Reaction time: 4×30 min (5 min intervals). <sup>f</sup>Reaction was performed in CH<sub>2</sub>Cl<sub>2</sub> (2 ml) in the dark. <sup>g</sup>Irradiation under blue light. ND, not detected.

In the context of exploring novel avenues in photo-mechanochemistry, mechanoluminescent (ML) materials have emerged as a promising lead. Although ML materials have found widespread use in biological applications as stress sensors, their application in organic synthesis remains largely untapped. Given that ML materials can emit photons when subjected to mechanical force<sup>35–41</sup>, we hypothesize that by mixing them with reactants and milling them together, mechanical energy can be converted into light energy, thereby generating excited-state molecules, and facilitating other thermally activated reaction steps in solid-state synthetic transformations. This notion suggests a possible mechano-photoexcitation strategy (Fig. 1d). Pioneering works by Xu and co-workers utilized mechanical stimulation to activate SrAl<sub>2</sub>O<sub>4</sub>:Eu<sup>2+</sup> (SAOE) and CaYAl<sub>3</sub>O<sub>7</sub>:Eu<sup>2+</sup> (CYAE), resulting in sustainable illumination and achieving the photoexcitation of TiO<sub>2</sub> nanoparticles and the fluorescent probe molecule fluorescein<sup>42–44</sup>. Notably, SAOE and CYAE belong to elastico-mechanoluminescent materials, which exhibit non-destructive mechanoluminescence upon elastic deformation and emit photons repeatedly when subjected to mechanical force. This implies that elastico-mechanoluminescent materials can potentially offer uninterrupted luminescence for mechanochemical reactions under continuous mechanical stimulation<sup>35,39,40</sup>. In this work, we present the investigation into the utilization of ML materials in the context of a mechano-photoexcitation strategy, aiming to facilitate solid-state photochemical reactions without the need for an external light source. This research represents a promising frontier in the advancement of sustainable and efficient organic synthesis.

## Results and discussion

As a proof-of-concept, our initial aim was to achieve mechano-photoinduced homolytic cleavage of chemical bonds, a common strategy used to generate reactive radical intermediates for subsequent organic transformations<sup>45–47</sup>, using ML materials. One notable example is the visible-light-mediated Hofmann–Löffler–Freitag (HLF) reaction for constructing of N-heterocycles. This reaction is initiated by photoinduced homolytic cleavage of weak N–I bonds, which are generated in situ from amides using molecular iodine or iodide salts in the presence of excess hypervalent iodine oxidants<sup>48–50</sup>. Efficient photoexcitation of these chemical bonds is typically accomplished through illumination from fluorescent bulbs or light-emitting diode (LED) lamps. A study by Muniz and co-workers revealed that light sources within the 400–600 nm wavelength range are effective in inducing N–I bond cleavage (N–I bond dissociation energy = 38.0 kcal mol<sup>−1</sup>)<sup>51–53</sup>.

Consequently, we selected several commercially available ML materials with emission wavelengths aligned with the required wavelength to explore mechanical HLF reactions. These materials include ZnS:Cu<sup>+</sup> (λ<sub>ML</sub> = 517 nm), SrAl<sub>2</sub>O<sub>4</sub>:Eu<sup>2+</sup> (λ<sub>ML</sub> = 520 nm), SrAl<sub>2</sub>O<sub>4</sub>:Eu<sup>2+</sup>/Dy<sup>3+</sup> (λ<sub>ML</sub> = 516 nm), Sr<sub>2</sub>MgSi<sub>2</sub>O<sub>7</sub>:Eu<sup>2+</sup>/Dy<sup>3+</sup> (λ<sub>ML</sub> = 460 nm), SrSi<sub>2</sub>O<sub>2</sub>N<sub>2</sub>:Eu<sup>2+</sup> (λ<sub>ML</sub> = 498 nm) and BaSi<sub>2</sub>O<sub>2</sub>N<sub>2</sub>:Eu<sup>2+</sup> (λ<sub>ML</sub> = 498 nm)<sup>37–39</sup>. We conducted the preliminary reaction screening with sulfonamide **1a**, sodium iodide (1 equiv.) and PhI(OCOCF<sub>3</sub>)<sub>2</sub> (4 equiv.) in the presence of different ML powders (100 wt%). The experiments were performed using a Retsch MM 400 mixer mill equipped with a 5 ml stainless-steel milling jar and twenty 3-mm-diameter stainless-steel balls. Gratifyingly, the desired product **2a** was obtained with all ML materials in yields ranging from

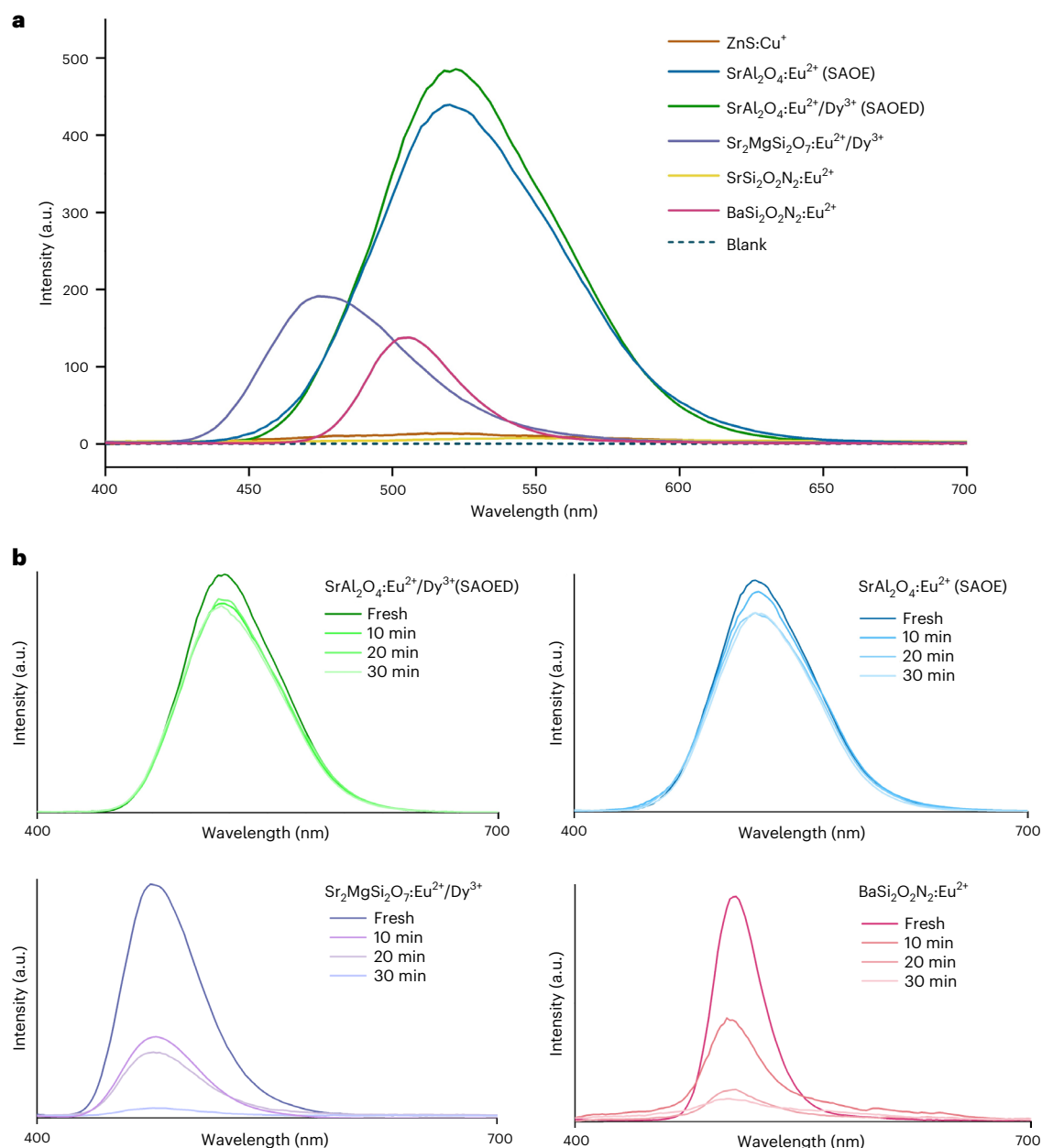


**Fig. 2 | Mechanoluminescence spectra. a**, ML spectra of different materials (under a 20 N mechanical stimulus). **b**, ML spectra after milling.

16% to 49%;  $\text{SrAl}_2\text{O}_4:\text{Eu}^{2+}/\text{Dy}^{3+}$  (SAOED) demonstrated the highest performance (Table 1, entries 1–6). Further evaluation of oxidants indicated that Koser's reagent,  $\text{PhI}(\text{OH})\text{OTs}$  (Ts, tosyl), provided the best results, yielding **2a** in a 63% yield (entries 7–9). The addition of 4 equiv. of  $\text{Na}_2\text{CO}_3$  significantly improved the yield to 84%, whereas  $\text{Al}_2\text{O}_3$  and  $\text{SiO}_2$  showed no benefits (entries 10–12)<sup>6,7,15,16</sup>. This improvement was probably due to  $\text{Na}_2\text{CO}_3$  acting as a base, facilitating the final step of the reaction by deprotonating the N–H bond and enabling the subsequent intramolecular  $\text{S}_{\text{N}}2$  substitution. The investigation into the impact of ball quantity and size on the ball-milling process (entries 13 and 14) revealed that multiple smaller balls, when used in a comparable total mass, outperform a single larger ball in terms of reaction efficiency. This enhanced efficiency is probably due to the low trigger threshold of SAOED, which allowed even smaller balls to effectively induce luminescence<sup>38</sup>. Although larger balls might generate more intense ML emission per impact, their lower impact frequency reduced the overall reaction efficiency. Conversely, the increased number of smaller balls

led to more frequent impacts and better distribution of mechanical energy, enhancing the overall mechano-photoexcitation efficiency. Shortened milling duration resulted in significantly reduced yields. Extended milling times did not lead to improved yields and, in fact, decreased efficiency (entries 15 and 16). This decline was probably due to heat accumulation during prolonged milling, leading to side reactions or product decomposition. To counter this issue, the milling process was adjusted to four 30 min intervals with 5 min breaks in between to reduce heat accumulation (entry 17). As a result, the optimized milling protocol resulted in a yield of 90%. Control experiments showed that without SAOED, **2a** could only be obtained in a 9% yield (entry 18). Subsequently, we performed the reaction in a dichloromethane solution without ML materials, with no product detected in the absence of light, whereas 88% of **2a** was obtained upon irradiation with a blue LED lamp (entry 19).

To further understand the varying performance of different materials in the HLF reaction, we conducted a comparative analysis of the

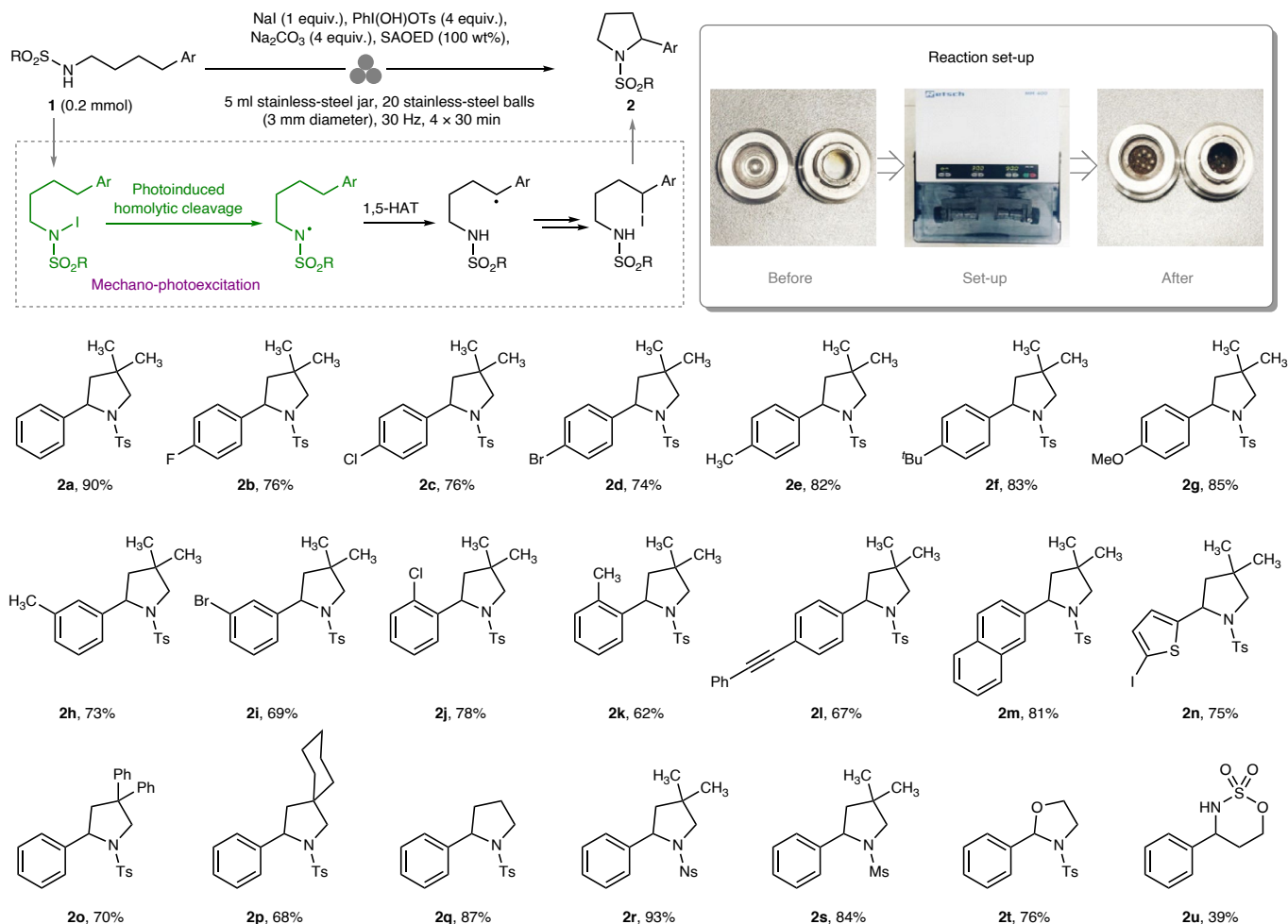


**Fig. 3 | Mechanochemical HLF reaction.** Reaction set-up and substrate scope. HAT, hydrogen-atom transfer.

mechanoluminescence intensities of these materials under a 20 N mechanical stimulus, using a method adapted from the literature (Supplementary Figs. 2 and 3)<sup>54</sup>. The results showed that SAOE and SAOED significantly outperformed other ML materials, with SAOED demonstrating the best performance (Fig. 2a). Additionally, we examined the ML spectra of several ML powders subjected to ball milling for different durations using the aforementioned method. After 30 min and 20 min of milling,  $\text{Sr}_2\text{MgSi}_2\text{O}_7\text{:Eu}^{2+}/\text{Dy}^{3+}$  and  $\text{BaSi}_2\text{O}_7\text{:Eu}^{2+}$ , respectively, exhibited noticeable luminescence decay, whereas SAOE and SAOED displayed significantly lower degrees of decay (Fig. 2b). These findings are consistent with the observed efficiency of these ML materials in the HLF reactions (Table 1).

With the optimal reaction conditions in hand, we explored the substrate scope of this mechanochemical method. As illustrated in Fig. 3, both electron-donating and electron-withdrawing substituents were well tolerated, yielding the corresponding pyrrolidines **2a–2k** in moderate to high yields (62–90%). Even with 4-(phenylethynyl) phenyl and 2-naphthyl groups, the  $\delta$ -amination process remained efficient, furnishing heterocycles **2l** and **2m** with yields of 67% and 81%, respectively. Sulfonamide containing a heterocyclic group was also examined. Pyrrolidine **2n**, which was generated through a combination of HLF process and in situ electrophilic iodination of the thiophene group, was isolated with a 75% yield. Variations of substituents on the alkyl chain were explored, leading to the formation of products (**2o–q**), and the reaction proceeded equally well with unsubstituted alkyl chains. Changing the protecting group on the nitrogen atom to nosyl (Ns) and mesyl (Ms) groups did not significantly affect the

synthetic transformation (**2r** and **2s**). Furthermore, oxazolidine **2t** and oxathiazine dioxide **2u** were synthesized successfully using our mechanochemical process.

To expand the scope of mechano-photoexcitation strategies in organic synthesis, we aimed to apply this mechano-photoactivation strategy using ML materials to excite EDA complexes in synthetic transformations, thus enabling greener photocatalytic synthetic chemical processes<sup>55,56</sup>. For our investigation, we selected Li and co-worker's work on a triarylamine–sulfonyl chloride EDA complex in photocatalytic sulfonylation reactions as a model<sup>57</sup>. Upon photon excitation, the EDA complex undergoes a SET, forming an amine radical cation and a sulfonyl chloride radical anion pair. Subsequently, the sulfonyl chloride radical anion decomposes into chloride ions and sulfonyl radicals, which then add to alkenes to form the desired product (Fig. 4a).

Extensive optimization studies revealed that milling 4-toluenesulfonyl chloride **3a**, 1,1-diphenylethylene **4a**, tris-(4-methoxyphenyl)amine (10 mol%) and SAOED (100 wt%) at a frequency of 30 Hz provided the desired product **5a** in 89% yield (Fig. 4b). Performing the reaction under aerobic conditions resulted in a decreased yield of 27%, possibly due to oxygen reacting with the highly sensitive radical intermediates in the reaction<sup>57</sup>. Additionally, the inclusion of various salt additives did not enhance the reaction, and adding MeCN as a liquid-assisted grinding agent completely inhibited the EDA reaction. Furthermore, using larger but fewer milling balls resulted in lower yields compared with using smaller but more numerous balls, similar to observations in the HLF reaction. Omitting SAOED failed to produce the desired product. With the optimal conditions in hand, we

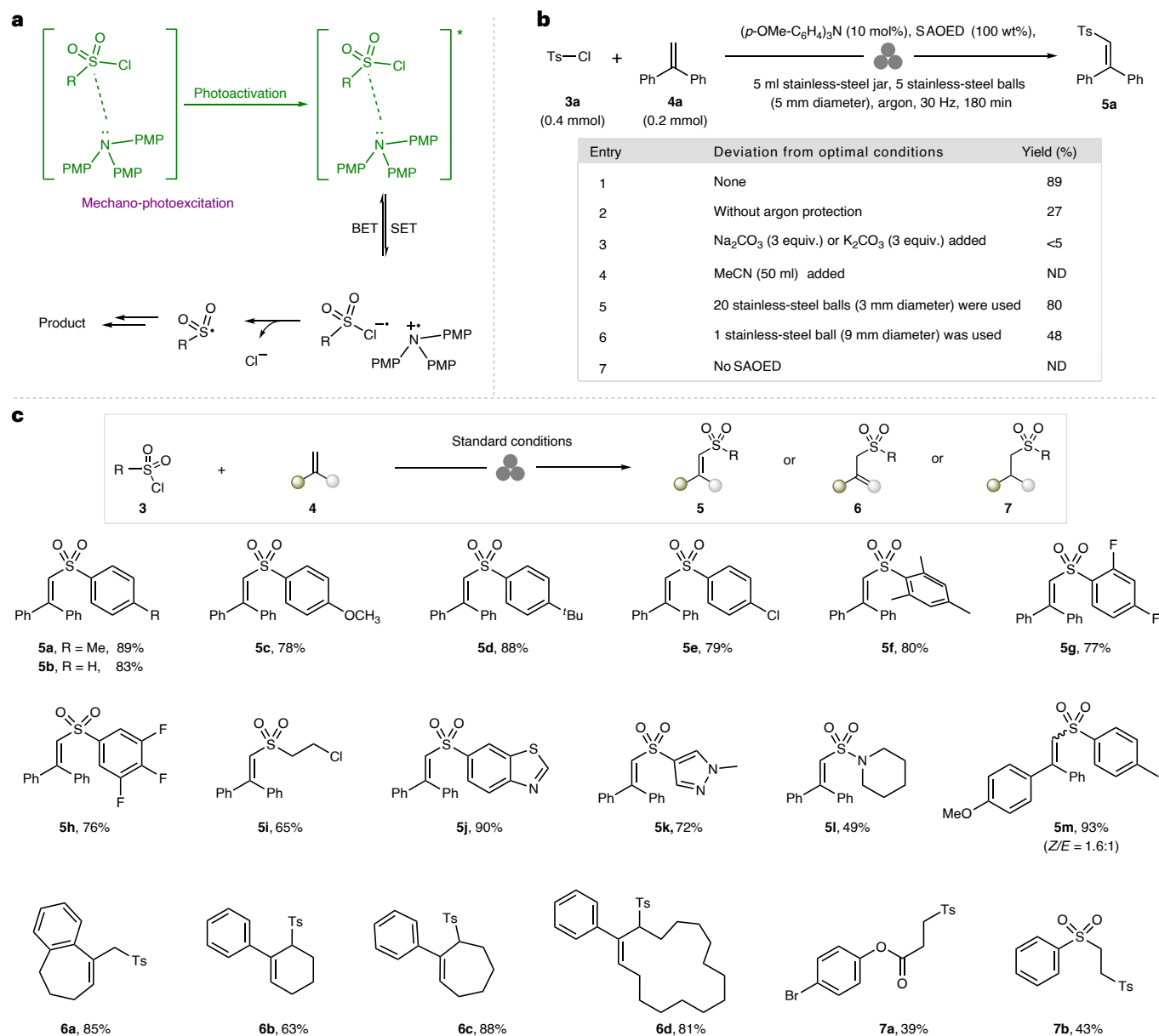


**Fig. 4 | Mechanochemical sulfonylation reaction. a**, Mechano-photoexcitation of the EDA complex. **b**, Optimized conditions and controls. **c**, Substrate scope. ND, not determined. PMP, 4-methoxyphenyl. Isolated yields are shown unless otherwise noted. 1,4-Cyclohexadiene (0.8 mmol) was used as a reducing agent in the preparation of compounds **7a** and **7b**. Z/E refers to Z/E isomerism.

investigated the scope of this mechanochemical sulfonylation reaction. A series of alkenyl sulfones **5** and allyl sulfones **6** with significant synthetic value were formed with moderate to good yields of 49–93% (Fig. 4c). Moreover, hydrosulfonylation of alkenes was accomplished by adding 1,4-cyclohexadiene as the reductant, resulting in the formation of **7a** and **7b**.

Next, we investigated the mechanisms underlying the mechanical photochemical process. The involvement of a radical pathway in the reaction was supported by the inhibition of the catalytic EDA reaction with the addition of TEMPO ((2,2,6,6-tetramethylpiperidin-1-yl)oxyl, a radical scavenger). In a ‘radical clock’ experiment with cyclopropyl-containing substrate **4n** under standard conditions, the formation of ring-opened product **8**, along with product **5n**, indicates the presence of an  $\alpha$ -cyclopropyl radical intermediate, which undergoes ring-opening and further rearrangement to yield product **8** (Fig. 5a). These results demonstrate that the reaction follows a radical pathway, which is consistent with the mechanism reported in solution

conditions<sup>57</sup>. We also explored further practical applications of this strategy. Scaling up the mechanical catalytic sulfonylation reaction to gramme quantities was accomplished by extending the reaction time and utilizing larger jars (Fig. 5b).

Characterization of ML materials was conducted before and after the reaction to observe any changes. Scanning electron microscopy (SEM) analysis of fresh commercially available SAOED powders showed clear particle shapes (Fig. 5c). The SEM image of recycled SAOED, which was utilized in the EDA reaction, revealed deformation in particle morphology, along with a reduction in particle size. This observation indicates that the mechanical stimulation of ball milling was exerted on the SAOED materials. Additionally, powder X-ray diffraction (PXRD) analysis, which was used to determine the crystalline phase composition, showed nearly identical patterns for SAOED before and after ball milling, with sharp, high-intensity peaks. This result implies that the crystalline phase of SAOED remains unaltered despite the mechanical forces during milling (Fig. 5d). Additionally, the recyclability of SAOED

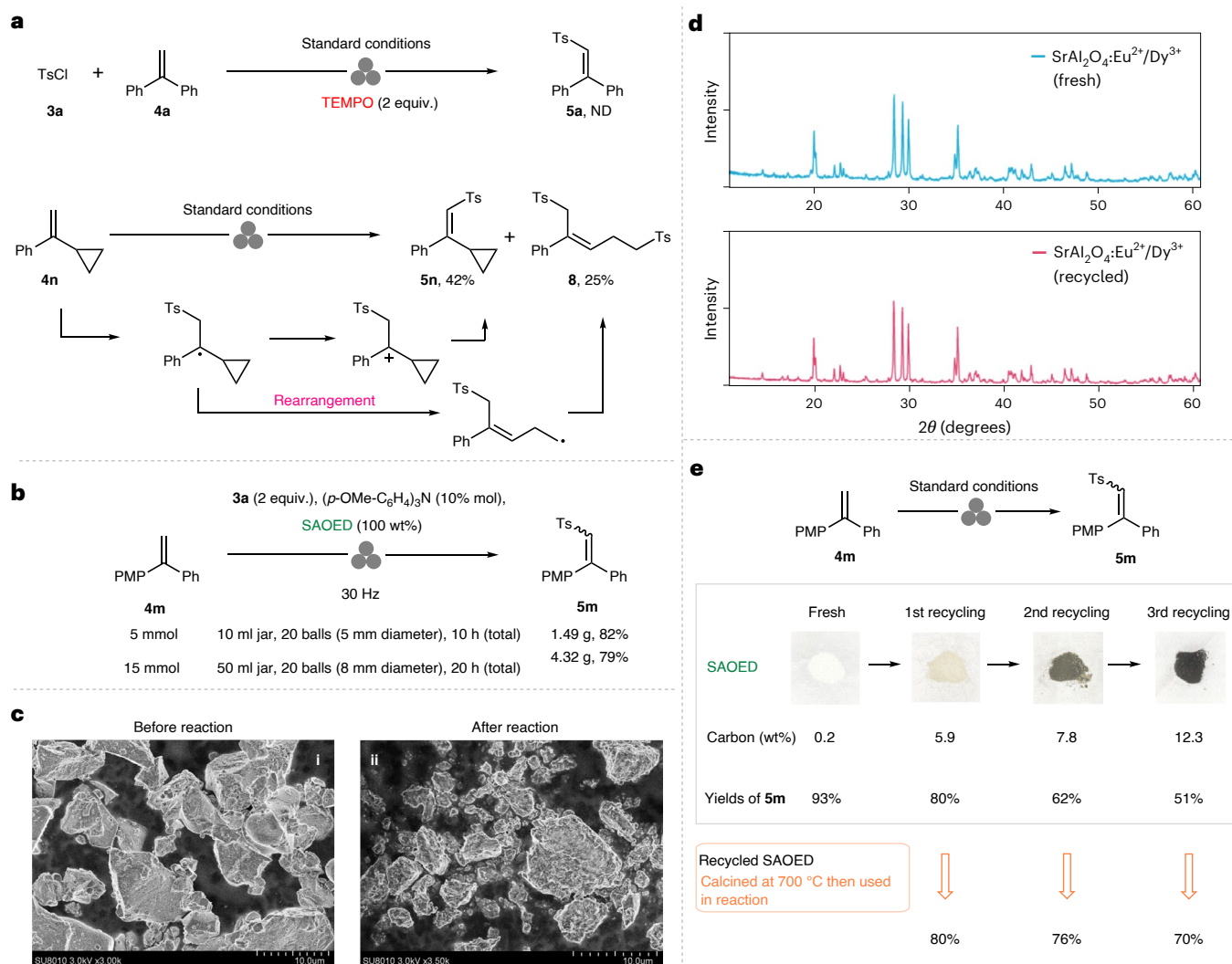


**Fig. 5 | Mechanistic studies, gramme-scale synthesis and ML material recycling.** **a**, Radical scavenger experiment and radical clock experiment. **b**, Gramme-scale synthesis. **c**, SEM images of SAOED materials before and after sulfonation reaction. **d**, PXRD patterns of SAOED materials. **e**, SAOED recycling experiments.

particles was investigated. After separating them from the reaction mixture by filtration through filter paper, thoroughly washing with ethyl acetate and dichloromethane, and drying in an oven, SAOED can be reused for sulfonation reactions under the same conditions. However, a decrease in yield was observed after each cycle (Fig. 5e). Carbon determination experiments indeed revealed a significant increase in the carbon content of the recovered SAOED, which probably accounts for the observed decline in yields during the recycling experiments. Attempts to remove the organic substances adsorbed on the surface of the SAOED powder using various organic solvents were ineffective. Notably, some SAO-based materials have been reported to exhibit self-reproducibility after annealing<sup>38,39,41</sup>. We therefore hypothesized that calcination could not only remove organic residual from SAOED but also enhance its reproducibility. To test this hypothesis, we subjected the recovered SAOED to calcination in a tube furnace under an air atmosphere at 700 °C for 2 h. The calcined SAOED, when reintroduced into the reaction, exhibited improved yields compared with its uncalcined counterpart. This approach demonstrates a promising method for recycling SAOED, enhancing its sustainability and extending its operational lifespan in mechanochemical reactions.

To further validate the involvement of mechano-photoactivation process with ML materials in the transformations, a series of control experiments were conducted. Considering that SAOED exhibits

piezoelectric properties<sup>37</sup>, it is possible that radical intermediates could be generated through SET process in the mechano-redox strategy<sup>32</sup>. To probe this, we replaced SAOED with piezoelectric materials such as BaTiO<sub>3</sub>, LiNbO<sub>3</sub> and ZnO in the sulfonation reaction. The results revealed that none of these piezoelectric materials could facilitate the reaction, with the majority of the starting materials remained unreacted (Fig. 6a). Furthermore, no product was obtained when oxides, such as Al<sub>2</sub>O<sub>3</sub>, SrO and SiO<sub>2</sub>, were used instead of SAOED. Conversely, other ML materials successfully promoted the reaction, albeit with reduced yields, strongly supporting the notion of mechano-photoactivation. As Bolm and co-workers have demonstrated that sulfur radicals can be generated via the homolytic cleavage of the sulfur–chlorine bond in sulfoximidoyl chloride purely through mechanical force in a stainless-steel ball-mill device<sup>58</sup>, we conducted control experiments to assess the contribution of stainless-steel materials to radical generation in our mechanical sulfonation reactions (Fig. 6b). In the absence of SAOED, the sulfonation reaction failed to proceed in the stainless-steel jar/balls. Additionally, in the presence of SAOED, the use of a ZrO<sub>2</sub> jar and ZrO<sub>2</sub> balls resulted in the formation of product 5a in 10% yield, whereas no product formation was observed when the reaction was conducted in a polytetrafluoroethylene (PTFE) jar with ZrO<sub>2</sub> balls. To explore the potential influence of trace metal catalysts from the stainless-steel vessels, the reaction mixture was supplemented with 10% iron powder

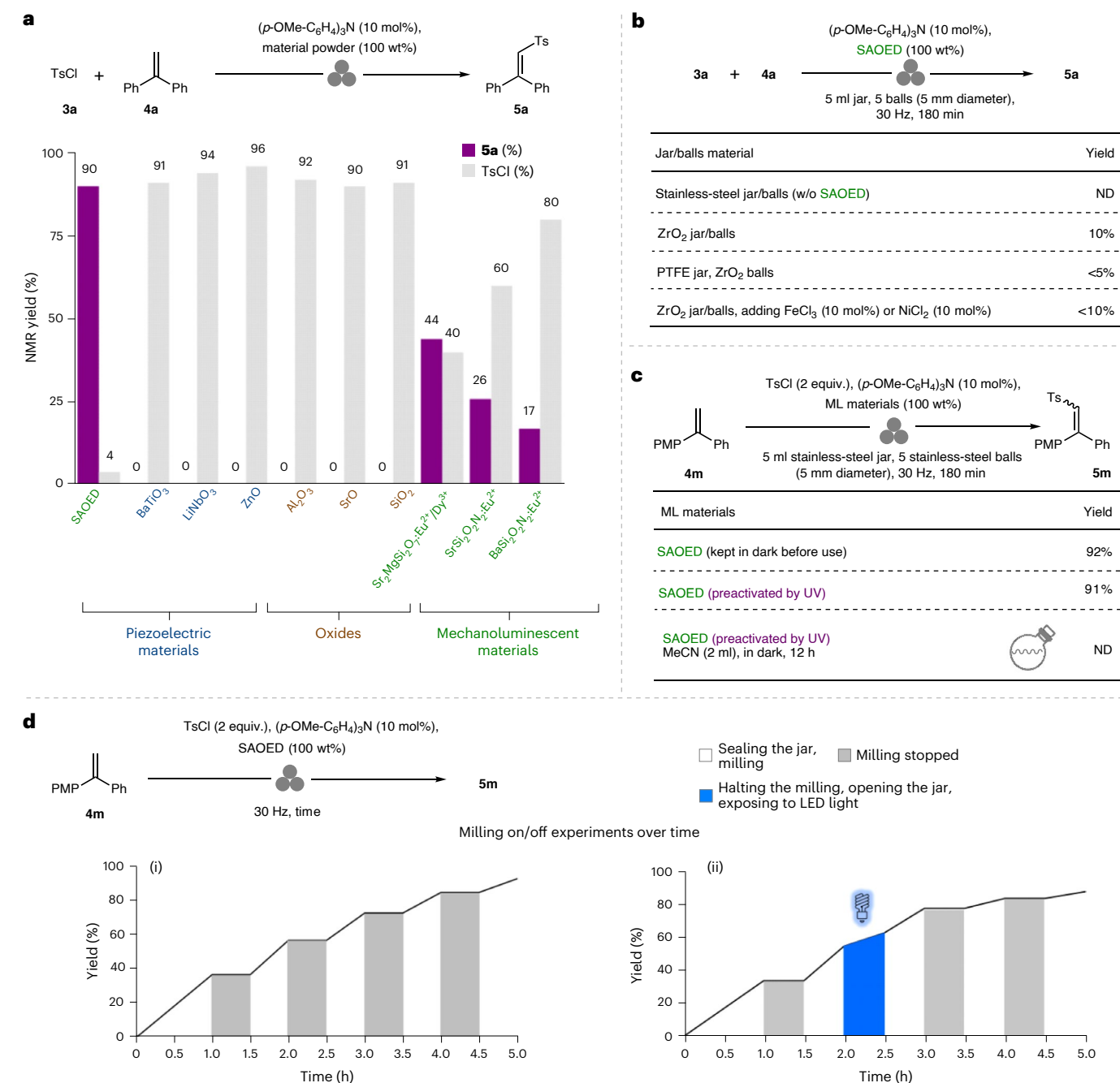


**Fig. 6 | Control experiments. a**, Effect of material piezoelectric properties on sulfonylation reactions. **b**, Investigation of stainless-steel-initiated radical generation. **c**, Influence of SAOED photoluminescence on reactions. **d**, Milling on/off experiments. w/o, without.

or 10% NiCl<sub>2</sub> additives when using ZrO<sub>2</sub> jar/balls. These additives did not enhance the reaction, ruling out the impact of trace metal catalysts from stainless-steel vessels on the reaction. These results not only emphasized the critical role of SAOED but also indicated that the materials of the jar and balls could significantly affect the reaction process. The elastic moduli of the jar and ball materials, acting as friction media, may influence the stimulation on SAOED, potentially affecting its mechanoluminescence during the reaction<sup>36</sup>. Furthermore, the composition of the jar and balls might affect the efficiency of other steps in mechanochemical reactions<sup>71</sup>.

As a commercially available long phosphorescent phosphor, SAOED exhibits photoluminescence properties<sup>37,59</sup>, implying its potential to be preactivated by ambient light and emit photons without the need for mechanical activation. To explore the role of continuous

mechanical stimulation in our reactions, several control experiments were performed. Keeping SAOED in the dark for 48 h before the sulfonylation reaction gave a 92% product yield under standard conditions. In comparison, exposing SAOED to ultraviolet light irradiation for 2 h prior to the reaction resulted in a 91% yield. However, conducting the reaction in acetonitrile solution in the dark using preactivated SAOED as the light source resulted in no reaction (Fig. 6c). To further investigate the impact of SAOED afterglow emission on photoexcitation, we performed milling on-off experiments, which revealed that product formation ceased when milling was paused, but resumed when milling was resumed (Fig. 6d). However, upon halting the milling process, opening the milling jar and exposing the reaction mixture to LED light for 30 min, we observed sustained reaction progression during this period. Additionally, ultraviolet-visible study results showed that the



ML emission wavelength range of SAOED satisfied the requirements for exciting HLF reactions and EDA reactions. (Supplementary Figs. 9–11). Although we could not fully rule out the contribution of photoluminescence and afterglow luminescence to the reactions, the data show that they have little effect on the yield. These results also underscore the necessity of continuous mechanical-stimulation-induced ML emission during the reaction process.

## Conclusion

We present a mechano-photoexcitation strategy harnessing ML materials as continuous photon emitters under sustained and non-destructive mechanical activation. This mechano-photoexcitation strategy employs SAOED as an ML material, facilitating the photoinduced HLF reaction and EDA complex photoactivation, both without the need for excessive solvents and external light sources. This strategy not only complements the mechanoredox strategy, whereby piezoelectric materials are mechanically activated to serve as catalysts for SET processes, but also offers a new perspective on integrating mechanochemistry and photochemistry. By harnessing the emission characteristics of SAOED ( $\lambda_{\text{max}} = 520 \text{ nm}$ ), this strategy offers a promising avenue for adapting green-light-promoted (>500 nm) chemical reactions to mechanochemical platforms. Potential applications could extend beyond the direct excitation of green-light-absorbing reactants and complexes, and include reactions catalysed by a diverse array of green-light-sensitive catalysts<sup>60–64</sup>, such as small-molecule catalysts (eosin Y and rhodamine 6G), metal catalysts ( $\text{Fe}(\text{btz})_3$  and  $\text{Cp}_2\text{TiCl}_2$ ,  $\text{btz}$ , 3,3'-dimethyl-1,1'-bis(*p*-tolyl)-4,4'-bis(1,2,3-triazol-5-ylidene); Cp, cyclopentadienyl), and heterogeneous catalysts ( $\text{CdS}/\text{CdSe}$  and  $\text{AuNP}@/\text{TiO}_2$ ). The versatility of this approach opens new possibilities for mechanochemical synthesis.

## Methods

### Mechanochemical HLF reaction

To a 5 ml stainless-steel-milling jar containing twenty 3-mm-diameter stainless-steel balls, sulfonamide (**1**, 0.2 mmol), NaI (30.0 mg, 0.2 mmol, 1 equiv.),  $\text{PhI}(\text{OH})(\text{OTs})$  (313.8 mg, 0.8 mmol, 4 equiv.),  $\text{Na}_2\text{CO}_3$  (85.8 mg, 0.2 mmol, 1 equiv.) and SAOED (<15  $\mu\text{m}$ , 100 wt%) were added. The jar was then closed and placed in a ball mill (Retsch MM 400). The mechanochemical reaction was carried out for four periods of 30 min each at a frequency of 30 Hz. After milling, the reaction mixture was passed through a short silica-gel column eluting with ethyl acetate, and the filtrate was evaporated to dryness. The corresponding product was then isolated via column chromatography on silica gel or preparative thin-layer chromatography.

### Mechanochemical sulfonylation reaction

In a glovebox, sulfonyl chloride (**3**, 0.4 mmol, 2 equiv.), alkene (**4**, 0.2 mmol, 1 equiv.), (*p*-OMe- $\text{C}_6\text{H}_4$ )<sub>3</sub>N (6.7 mg, 0.02 mmol) and SAOED (<15  $\mu\text{m}$ , 100 wt%) were added to a 5 ml stainless-steel milling jar containing five 5-mm-diameter stainless-steel balls. The jar was then closed inside the glovebox and placed in a ball mill (Retsch MM 400). The mechanochemical reaction was carried out for 180 min at a frequency of 30 Hz. After milling, the reaction mixture was passed through a short silica-gel column eluting with ethyl acetate, and the filtrate was evaporated to dryness. The corresponding product was then isolated via column chromatography on silica gel or preparative thin-layer chromatography.

### Mechanochemical hydrosulfonylation reaction

In a glovebox, alkene (**4**, 0.2 mmol, 1 equiv.),  $\text{TsCl}$  (66.7 mg, 0.4 mmol, 2 equiv.), (*p*-OMe- $\text{C}_6\text{H}_4$ )<sub>3</sub>N (6.7 mg, 0.02 mmol), 1,4-cyclohexadiene (64.1 mg, 0.8 mmol, 4 equiv.) and SAOED (<15  $\mu\text{m}$ , 100 wt%) were added to a 5 ml stainless-steel milling jar containing twenty 3-mm-diameter stainless-steel balls. The jar was then closed inside the glovebox and placed in a ball mill (Retsch MM 400). The mechanochemical reaction

was carried out for 180 min at a frequency of 30 Hz. After milling, the reaction mixture was passed through a short silica-gel column eluting with ethyl acetate, and the filtrate was evaporated to dryness. The corresponding product was then isolated via column chromatography on silica gel or preparative thin-layer chromatography.

## Data availability

All data supporting the findings of this study are available within the article and its Supplementary Information. Source data are provided with this paper.

## References

- Hoffmann, N. Photochemical reactions as key steps in organic synthesis. *Chem. Rev.* **108**, 1052–1103 (2008).
- Kärkäs, M. D., Porco, J. A. Jr. & Stephenson, C. R. J. Photochemical approaches to complex chemotypes: applications in natural product synthesis. *Chem. Rev.* **116**, 9683–9747 (2016).
- Stephenson C., Yoon T., MacMillan D. W. C., *Visible Light Photocatalysis in Organic Chemistry* (Wiley, 2018).
- Prier, C. K., Rankic, D. A. & MacMillan, D. W. C. Visible light photoredox catalysis with transition metal complexes: applications in organic synthesis. *Chem. Rev.* **113**, 5322–5363 (2013).
- Crisenza, G. E. M. & Melchiorre, P. Chemistry glows green with photoredox catalysis. *Nat. Commun.* **11**, 803 (2020).
- Martinez, V., Stolar, T., Karadeniz, B., Brekalo, I. & Užarević, K. Advancing mechanochemical synthesis by combining milling with different energy sources. *Nat. Rev. Chem.* **7**, 51–65 (2023).
- Do, J. L. & Friščić, T. Mechanochemistry: a force of synthesis. *ACS Central Sci.* **3**, 13–19 (2017).
- Boulatov, R. (ed.) *Polymer Mechanochemistry*, Vol. 369, 209–238 (Springer, 2015).
- Garay, A. L., Pichon, A. & James, S. L. Solvent-free synthesis of metal complexes. *Chem. Soc. Rev.* **36**, 846–855 (2007).
- Friščić, T. New opportunities for materials synthesis using mechanochemistry. *J. Mater. Chem.* **20**, 7599–7605 (2010).
- James, S. L. et al. Mechanochemistry: opportunities for new and cleaner synthesis. *Chem. Soc. Rev.* **41**, 413–447 (2012).
- Patel, C. et al. Fluorochemicals from fluorspar via a phosphate-enabled mechanochemical process that bypasses HF. *Science* **381**, 302–306 (2023).
- Tan, D. & García, F. Main group mechanochemistry: from curiosity to established protocols. *Chem. Soc. Rev.* **48**, 2274–2292 (2019).
- Hernández, J. G. & Bolm, C. Altering product selectivity by mechanochemistry. *J. Org. Chem.* **82**, 4007–4019 (2017).
- Friščić, T., Mottillo, C. & Titli, H. M. Mechanochemistry for synthesis. *Angew. Chem. Int. Ed.* **132**, 1030–1041 (2020). (2017).
- Howard, J. L., Cao, Q. & Browne, D. L. Mechanochemistry as an emerging tool for molecular synthesis: what can it offer? *Chem. Sci.* **9**, 3080–3094 (2018).
- Andersen, J. & Mack, J. Mechanochemistry and organic synthesis: from mystical to practical. *Green Chem.* **20**, 1435–1443 (2018).
- Jones, A. C., Leitch, J. A., Raby-Buck, S. E. & Browne, D. L. Mechanochemical techniques for the activation and use of zero-valent metals in synthesis. *Nat. Syn.* **1**, 763–775 (2022).
- Sokolov, A. N., Bučar, D. K., Baltrusaitis, J., Gu, S. X. & MacGillivray, L. R. Supramolecular catalysis in the organic solid state through dry grinding. *Angew. Chem. Int. Ed.* **25**, 4273–4277 (2010).
- Stojaković, J., Farris, B. S. & MacGillivray, L. R. Liquid-assisted vortex grinding supports the single-step solid-state construction of a [2.2]paracyclophane. *Faraday Discuss.* **170**, 35–40 (2014).
- Elacqua, E., Kummer, K. A., Groeneman, R. H., Reinheimer, E. W. & MacGillivray, L. R. Post-application of dry vortex grinding improves the yield of a [2+2] photodimerization: addressing static disorder in a cocrystal. *J. Photoch. Photobio. A.* **331**, 42–47 (2016).

22. Liu, L. et al. Photo-thermo-mechanochemical approach to synthesize quinolines via addition/cyclization of sulfoxonium ylides with 2-vinylanilines catalyzed by iron (II) phthalocyanine. *Org. Lett.* **24**, 1146–1151 (2022).
23. Toda, F., Tanaka, K. & Sekikawa, A. Host–guest complex formation by a solid–solid reaction. *Chem. Commun.* **4**, 279–280 (1987).
24. Hernández, J. G. Mechanochemical borylation of aryl diazonium salts; merging light and ball milling. *Beilstein J. Org. Chem.* **13**, 1463–1469 (2017).
25. Obst, M. & König, B. Solvent-free, visible-light photocatalytic alcohol oxidations applying an organic photocatalyst. *Beilstein J. Org. Chem.* **12**, 2358–2363 (2016).
26. Obst, M., Shaikh, R. S. & König, B. Solvent-free coupling of aryl halides with pyrroles applying visible-light photocatalysis. *React. Chem. Eng.* **2**, 472–478 (2017).
27. Štrukil, V. & Sajko, I. Mechanochemically-assisted solid-state photocatalysis (MASSPC). *Chem. Commun.* **53**, 9101–9104 (2017).
28. Biswas, S. et al. Photomechanochemical control over stereoselectivity in the [2+2] photodimerization of acenaphthylene. *Faraday Discuss.* **241**, 266–277 (2023).
29. Baier, D. M., Spula, C., Fanenstich, S., Grätz, S. & Borchardt, L. The regioselective solid-state photo-mechanochemical synthesis of nanographenes with UV light. *Angew. Chem. Int. Ed.* **62**, e202218719 (2023).
30. Millward, F. & Zysman-Colman, E. Mechanophotocatalysis: a generalizable approach to solvent-minimized photocatalytic reactions for organic synthesis. *Angew. Chem. Int. Ed.* **63**, e202316169 (2024).
31. Kubota, K., Pang, Y., Miura, A. & Ito, H. Redox reactions of small organic molecules using ball milling and piezoelectric materials. *Science* **366**, 1500–1504 (2019).
32. Pang, Y., Lee, J. W., Kubota, K. & Ito, H. Solid-state radical C–H trifluoromethylation reactions using ball milling and piezoelectric materials. *Angew. Chem. Int. Ed.* **59**, 22570–22576 (2020).
33. Amer, M. M., Hommelshheim, R., Schumacher, C., Kong, D. & Bolm, C. Electro-mechanochemical approach towards the chloro sulfoximidations of allenes under solvent-free conditions in a ball mill. *Faraday Discuss.* **241**, 79–90 (2023).
34. Schumacher, C., Hernández, J. G. & Bolm, C. Electro-mechanochemical atom transfer radical cyclizations using piezoelectric BaTiO<sub>3</sub>. *Angew. Chem. Int. Ed.* **59**, 16357–16360 (2020).
35. Xie, Y. & Li, Z. Triboluminescence: recalling interest and new aspects. *Chem* **4**, 943–971 (2018).
36. Zhuang, Y. & Xie, R.-J. Mechanoluminescence rebrighting the prospects of stress sensing: a review. *Adv. Mater.* **33**, 2005925 (2021).
37. Feng, A. & Smet, P. F. A review of mechanoluminescence in inorganic solids: compounds, mechanisms, models and applications. *Materials* **11**, 484 (2018).
38. Zhang, J.-C., Wang, X., Marriott, G. & Xu, C.-N. Trap-controlled mechanoluminescent materials. *Prog. Mater. Sci.* **103**, 678–742 (2019).
39. Zhang, H., Wei, Y., Huang, X. & Huang, W. Recent development of elasto-mechanoluminescent phosphors. *J. Lumin.* **207**, 137–148 (2019).
40. Jha, P. & Chandra, B. P. Survey of the literature on mechanoluminescence from 1605 to 2013. *Luminescence* **29**, 977–993 (2014).
41. Chandra, B. P. Development of mechanoluminescence technique for impact studies. *J. Lumin.* **131**, 1203–1210 (2011).
42. Terasaki, N., Zhang, H., Imai, Y., Yamada, H. & Xu, C.-N. Hybrid material consisting of mechanoluminescent material and TiO<sub>2</sub> photocatalyst. *Thin Solid Films* **518**, 473–476 (2009).
43. Terasaki, N., Yamada, H. & Xu, C.-N. Ultrasonic wave induced mechanoluminescence and its application for photocatalysis as ubiquitous light source. *Catal. Today* **201**, 203–208 (2013).
44. Terasaki, N., Zhang, H., Yamada, H. & Xu, C.-N. Mechanoluminescent light source for a fluorescent probe molecule. *Chem. Commun.* **47**, 8034–8036 (2011).
45. Protti, S., Ravelli, D. & Fagnoni, M. Designing radical chemistry by visible light-promoted homolysis. *Trends Chem.* **4**, 305–317 (2022).
46. Lang, Y., Li, C. J. & Zeng, H. Photo-induced transition-metal and external photosensitizer-free organic reactions. *Org. Chem. Front.* **8**, 3594–3613 (2021).
47. Sumida, Y. & Ohmiya, H. Direct excitation strategy for radical generation in organic synthesis. *Chem. Soc. Rev.* **50**, 6320–6332 (2021).
48. Wolff, M. E. Cyclization of N-halogenated amines (the Hofmann–Löffler reaction). *Chem. Rev.* **63**, 55–64 (1963).
49. Dorta, R. L., Francisco, C. G. & Suárez, E. Hypervalent organoiodine reagents in the transannular functionalisation of medium-sized lactams: synthesis of 1-azabicyclo compounds. *Chem. Commun.* 1168–1169 (1989).
50. Stateman, L. M., Nakafuku, K. M. & Nagib, D. A. Remote C–H functionalization via selective hydrogen atom transfer. *Synthesis* **50**, 1569–1586 (2018).
51. Martínez, C. & Muñoz, K. An iodine-catalyzed Hofmann–Löffler reaction. *Angew. Chem. Int. Ed.* **54**, 8287–8291 (2015).
52. Wappes, E. A., Fosu, S. C., Chopko, T. C. & Nagib, D. A. Triiodide-mediated  $\delta$ -amination of secondary C–H bonds. *Angew. Chem. Int. Ed.* **55**, 9974–9978 (2016).
53. Dean, J. A. & Lange, N. A. *Lange’s Handbook of Chemistry*, 15th edn (McGraw-Hill, 1999).
54. Sakai, K., Koga, T., Imai, Y., Maehara, S. & Xu, C.-N. Observation of mechanically induced luminescence from microparticles. *Phys. Chem. Chem. Phys.* **8**, 2819–2822 (2006).
55. Crisenza, G. E., Mazzarella, D. & Melchiorre, P. Synthetic methods driven by the photoactivity of electron donor–acceptor complexes. *J. Am. Chem. Soc.* **142**, 5461–5476 (2020).
56. Wortman, A. K. & Stephenson, C. R. EDA photochemistry: mechanistic investigations and future opportunities. *Chem.* **9**, 2390–2415 (2023).
57. Lasso, J. D. et al. A general platform for visible light sulfonylation reactions enabled by catalytic triarylamine EDA complexes. *J. Am. Chem. Soc.* **146**, 2583–2592 (2024).
58. Kong, D., Amer, M. M. & Bolm, C. Stainless steel-initiated chloro sulfoximidations of allenes under solvent-free conditions in a ball mill. *Green Chem.* **24**, 3125–3129 (2022).
59. Matsuzawa, T., Aoki, Y., Takeuchi, N. & Murayama, Y. A new long phosphorescent phosphor with high brightness, SrAl<sub>2</sub>O<sub>4</sub>: Eu<sup>2+</sup>, Dy<sup>3+</sup>. *J. Electrochem. Soc.* **143**, 2670 (1996).
60. Srivastava, V., Singh, P. K. & Singh, P. P. Recent advances of visible-light photocatalysis in the functionalization of organic compounds. *J. Photochem. Photobiol., C* **50**, 100488 (2022).
61. Srivastava, V. & Singh, P. P. Retracted article: Eosin Y catalysed photoredox synthesis: a review. *RSC Adv.* **7**, 31377–31392 (2017).
62. Jang, Y. J. et al. Green-light-driven Fe(III)(btz)<sub>3</sub> photocatalysis in the radical cationic [4+2] cycloaddition reaction. *Org. Lett.* **24**, 4479–4484 (2022).
63. Zhang, Z. et al. Titanocenes as photoredox catalysts using green-light irradiation. *Angew. Chem. Int. Ed.* **59**, 9355–9359 (2020).
64. Gisbertz, S. & Pieber, B. Heterogeneous photocatalysis in organic synthesis. *ChemPhotoChem* **4**, 456–475 (2020).

## Acknowledgements

We thank C. Bolm for proofreading and providing helpful suggestions on preparing the paper. This work is supported by the National Natural Science Foundation of China (22201230, Han Wang) and the

Science and Technology Base and Talent Special Project of Guangxi (AD21220087, D.Z.).

### Author contributions

Han Wang conceived the concept. X.X. and Han Wang developed the mechanical HLF reactions. J.G., D.Z. and Han Wang developed the mechanical sulfonylation reactions. D.Z., J.W., H.T.A., R.W.T., Hui Wang, Y.L. and Y.C. designed the mechanistic investigations. X.X., J.G. and H.T.A. performed the control experiments. H.T.A., R.W.T., J.W. and Han Wang wrote the paper.

### Competing interests

The authors declare no competing interests.

### Additional information

**Supplementary information** The online version contains supplementary material available at <https://doi.org/10.1038/s44160-024-00681-8>.

**Correspondence and requests for materials** should be addressed to Jie Wu or Han Wang.

**Peer review information** *Nature Synthesis* thanks Eli Zysman-Colman, Sven Grätz and the other, anonymous, reviewer(s) for their contribution to the peer review of this work. Primary Handling Editor: Peter Seavill, in collaboration with the *Nature Synthesis* team.

**Reprints and permissions information** is available at [www.nature.com/reprints](http://www.nature.com/reprints).

**Publisher's note** Springer Nature remains neutral with regard to jurisdictional claims in published maps and institutional affiliations.

Springer Nature or its licensor (e.g. a society or other partner) holds exclusive rights to this article under a publishing agreement with the author(s) or other rightsholder(s); author self-archiving of the accepted manuscript version of this article is solely governed by the terms of such publishing agreement and applicable law.

© The Author(s), under exclusive licence to Springer Nature Limited 2024